6
Accurate Treatment of Solids with the HSE Screened Hybrid

Thomas M. Henderson, Joachim Paier, and Gustavo E. Scuseria

6.1
Introduction and Basics of Density Functional Theory

Theoretical predictions of electronic properties offer a clear complement to experimental investigations. However, these theoretical predictions are only as useful as they are accurate. Ideally, first-principles calculations of electronic properties in periodic systems would use some high level many-body technique such as coupled-cluster theory; however these methods are horrifically expensive and therefore have restricted applicability in practice. While simpler many-body methods such as GW theory are significantly less expensive, the computational burden they impose nevertheless restricts their scope. Therefore, we often must perforce resort to single-particle descriptions, which are less computationally expensive but of course also less reliable.

One important single-particle reference is the Hartree–Fock (HF) method. The HF density matrix variationally minimizes the HF energy, given by

$$E_{\mathrm{HF}} = \langle \Phi | T | \Phi \rangle + \int d\boldsymbol{r}\, n(\boldsymbol{r}) v_{\mathrm{ext}}(\boldsymbol{r}) + \frac{1}{2} \int d\boldsymbol{r}_1 d\boldsymbol{r}_2 \frac{n(\boldsymbol{r}_1) n(\boldsymbol{r}_2)}{r_{12}} + E_x^{\mathrm{HF}}[\gamma], \qquad (6.1)$$

where n is the density, γ the density matrix, $r_{12} = |\boldsymbol{r}_1 - \boldsymbol{r}_2|$, and $E_x^{\mathrm{HF}}[\gamma]$ is the nonlocal Fock exchange energy

$$E_x^{\mathrm{HF}}[\gamma] = -\frac{1}{2} \int d\boldsymbol{r}_1 d\boldsymbol{r}_2 \frac{\gamma(\boldsymbol{r}_1, \boldsymbol{r}_2) \gamma(\boldsymbol{r}_2, \boldsymbol{r}_1)}{r_{12}}. \qquad (6.2)$$

That is, HF takes the usual one-body terms and the Coulomb interaction between electrons and adds a (known) functional of the density matrix to describe exchange. We construct the wave function $|\Phi\rangle$, density and density matrix from HF orbitals, obtained from a reference system of noninteracting electrons in which the external potential is augmented by the Hartree potential

$$v_H(\boldsymbol{r}_1) = \int d\boldsymbol{r}_2 \frac{n(\boldsymbol{r}_2)}{r_{12}}, \qquad (6.3)$$

and by an additional nonlocal potential v_x^{HF} which accounts for the effects of the exchange interaction on the orbitals. This nonlocal potential is the functional derivative of the exchange energy E_x^{HF} with respect to the density matrix

$$\frac{\delta E_x^{HF}}{\delta \gamma(r_2, r_1)} = \langle r_1 | v_x^{HF} | r_2 \rangle = -\frac{\gamma(r_1, r_2)}{r_{12}}, \tag{6.4}$$

so that matrix elements of v_x^{HF} between two single-particle functions are

$$\langle \phi | v_x^{HF} | \psi \rangle = \int dr_1 dr_2 \langle \phi | r_1 \rangle \langle r_1 | v_x^{HF} | r_2 \rangle \langle r_2 | \psi \rangle = -\int dr_1 dr_2 \phi^*(r_1) \psi(r_2) \frac{\gamma(r_1, r_2)}{r_{12}}. \tag{6.5}$$

HF has some advantages which should not be forgotten. It is exact for one-electron systems and has no one-electron self-interaction. It also forms a variationally optimal starting point for many-body methods. The orbital energies in HF have a clean interpretation as ionization potentials and electron affinities (i.e., Koopmans' theorem holds), which justifies the use of HF band energy differences to predict the fundamental band gap (the difference between the ionization potential and electron affinity of the system). Numerically, however, the HF band energy difference is a poor predictor of the fundamental gap.

Unfortunately, the advantages of HF are generally outweighed by disadvantages. Because it neglects electron correlation effects entirely, HF is insufficiently accurate for most applications. It has an innate tendency to overly favor electronically localized states, a manifestation of its form of many-electron self-interaction [1–3]. Calculating the nonlocal exchange interaction is computationally demanding in solids. The nonlocal exchange interaction also prevents HF from describing metallic behavior [4].

For all of these reasons, the single-particle method of choice is usually Kohn–Sham (KS) density functional theory (DFT) [5–7], in which the energy is given by

$$E_{KS} = \langle \Phi | T | \Phi \rangle + \int dr n(r) v_{ext}(r) + \frac{1}{2} \int dr_1 dr_2 \frac{n(r_1) n(r_2)}{r_{12}} + E_{xc}^{KS}[n]. \tag{6.6}$$

In other words, KS-DFT includes the usual one-body terms and Coulomb interaction between electrons and describes many-body exchange–correlation effects with a functional $E_{xc}^{KS}[n]$ of the density alone. The density is obtained from a reference system of noninteracting electrons in which the external potential is augmented by the Hartree potential and by an additional local potential v_{xc}^{KS} which accounts for the effects of the exchange and correlation interactions on the orbitals. This local potential is the functional derivative of the exchange–correlation energy E_{xc}^{KS} with respect to the density.

In principle, the exchange component of E_{xc}^{KS} can be taken directly from HF, with the sole distinction being that the density matrix should be constructed from KS orbitals. The functional derivative to build v_x^{KS} would then yield the optimized effective potential (OEP) [8, 9] which is in some sense the best local variant of v_x^{HF}. However, numerical computation of the OEP can be challenging, particularly in

a gaussian basis set [10]. Numerous approximations to OEP can solve this problem [11–16], but all remain computationally quite demanding in extended systems because they must construct the nonlocal exchange operator. In practice, HF-type exchange is almost never used in a genuine KS calculation.

The chief difficulty in KS-DFT is the need to approximate E_{xc}^{KS} and υ_{xc}^{KS} in practical calculations. Typical density functional approximations (DFAs) include the local density approximation (LDA) and generalized gradient approximations (GGAs) such as the functional of Perdew, Burke, and Ernzerhof (PBE) [17]. These are examples of what we shall term semilocal functionals, in which the exchange–correlation potential and energy density at a point depend only on the density and possibly its derivatives at that point. In effect, they expand the exchange–correlation energy around the homogeneous electron gas result, though they include a rather general dependence on the density gradient which allows them to satisfy known constraints on E_{xc}^{KS} that the second-order gradient expansion violates. Alternatively, one can view GGAs as curing the second-order gradient expansion's violations of known constraints on the exchange–correlation hole [18, 19]. Meta-GGAs such as the TPSS functional of Tao, Perdew, Staroverov, and Scuseria [20] add dependence on the local kinetic energy density, but are also semilocal in character.

For simple solids, these semilocal functionals are reasonably accurate, presumably because their electron densities tend to be slowly varying and the homogeneous electron gas is thus a reasonable starting point. This accuracy, however, does not extend to the description of the band gap, which is severely underestimated. For more complicated systems which may include localized electronic states, magnetic effects, rapidly varying densities, or other complicating factors, semilocal functionals are generally inadequate. Alternative semilocal functionals such as PBEsol [21] and revTPSS [22] can be constructed, but while these yield better lattice parameters and bulk moduli than their parents (respectively, PBE and TPSS), they do not remedy the failures of semilocal DFT in systems with the foregoing features, nor do they yield correct band gaps. Formally, this is largely because semilocal functionals do not include the derivative discontinuity of exact KS (see below) [23].

One possible solution which is very successful in molecular systems is to use a global hybrid functional [24, 25], which mixes a fraction of nonlocal HF-type exchange with conventional semilocal exchange:

$$E_{xc}^{hybrid} = E_{xc}^{DFA} + c_{HF}(E_x^{HF} - E_x^{DFA}). \tag{6.7}$$

Common hybrids include the three-parameter B3LYP hybrid [26] and the non-empirical [27] PBEh global hybrid [28, 29]. It should be emphasized that hybrid calculations are almost always done in what is called the generalized Kohn–Sham (GKS) sense [30], in which the nonlocal exchange *energy* yields a nonlocal exchange *interaction*.

Unfortunately, as already mentioned, nonlocal exchange is problematic in solids. Therefore, Heyd, Scuseria, and Ernzerhof introduced the Heyd–Scuseria–Ernzerhof

(HSE) screened hybrid [31–35]. In HSE, the electron–electron interaction is split into a short-range part and a long-range part, as

$$\frac{1}{r_{12}} = \underbrace{\frac{\mathrm{erfc}(\omega r_{12})}{r_{12}}}_{\mathrm{SR}} + \underbrace{\frac{\mathrm{erf}(\omega r_{12})}{r_{12}}}_{\mathrm{LR}}, \tag{6.8}$$

with a screening parameter ω which in the latest (HSE06) variant of the functional is numerically $\omega = 0.11a_0^{-1}$ in terms of the Bohr radius a_0. The short-range part is treated as in the PBEh global hybrid – that is, it uses 25% short-range exact exchange and 75% short-range PBE exchange – while the long-range part is treated purely by PBE. As ω goes to 0, the short-range part dominates and HSE reduces to PBEh; as ω goes to infinity, the short-range part vanishes and HSE reduces to PBE. By screening the electron–electron interaction in this way, one vastly reduces the expense of calculating the exact exchange interaction. Note that while the exchange interaction is short range in nature, the range over which exact exchange is included is approximately $1/\omega \sim 9a_0$, allowing delocalization to nearest and next-nearest neighboring atoms, which admits some form of nonlocality into the model without including all of it. It is also worth noting that Savin introduced the concept of range-separation in DFT [36–38], though he suggested the use of nonlocal exchange in the long range where HSE includes it instead in the short range.

Remarkably, this simple adjustment to the PBEh global hybrid leads to a computationally affordable functional which is accurate for a wide variety of properties of solids. It is our purpose here to summarize what we believe are the key features of HSE and explain roughly why the functional works; for a more detailed review of the successes and failures of HSE, see Ref. [39]. We begin by discussing what is perhaps the most notable success of HSE (its ability to predict band gaps) in Section 6.2 before stepping back to more carefully consider the physics of screened exchange (SX) in Section 6.3. Section 6.4 discusses several applications of HSE, and we offer a few concluding remarks in Section 6.5.

6.2
Band Gaps

Probably the most important success of HSE is its ability to predict semiconductor band gaps from its band energy differences. Here, we want to rationalize this success and set up the discussion for what follows. Before we begin, however, we had best be precise about what we mean when we say that HSE accurately predicts band gaps.

The fundamental band gap of the system deals with the energy required to add or remove electrons. We define it as

$$\Delta E_{\mathrm{fg}}(N) = E(N+1) + E(N-1) - 2E(N), \tag{6.9}$$

where $E(N)$ is the energy of the N-electron system. The optical gap instead measures the energy required to excite an electron, and is just the lowest electronic excitation

energy of the system. The optical gap is lower than the fundamental gap by the exciton binding energy, which represents the interaction between the excited electron and the hole created upon excitation.

In HF, Koopmans' theorem tells us that the HF fundamental gap is just equal to the HF band energy difference. The HF optical gap can be computed from the time-dependent (TD) linear reponse (generally just known as TD HF) and is lower than the HF fundamental gap; in other words, HF predicts a nonzero exciton binding energy [40, 41]. Due to self-interaction in the unoccupied energy levels, the HF fundamental gap severely overestimates the experimental fundamental gap, at least for semiconductors and typical insulators.

In exact KS, we do not have Koopmans' theorem. However, we can use the Janak–Slater theorem instead [42]. We obtain the well-known result that the exact KS fundamental gap is

$$\Delta E_{\text{fg}}^{\text{KS}}(N) = \varepsilon_{N+1}^{\text{KS}}(N) - \varepsilon_{N}^{\text{KS}}(N) + \Delta_{\text{xc}}(N), \tag{6.10}$$

where $\Delta_{\text{xc}}(N)$ arises from the discontinuity in $v_{\text{xc}}^{\text{KS}}$ as a function of N at integer N [43, 44]. Standard semilocal functionals and hybrid functionals in the generalized KS sense do not exhibit this discontinuity [23], so their prediction for the fundamental gap is

$$\Delta E_{\text{fg}}^{\text{DFA}}(N) = \varepsilon_{N+1}^{\text{DFA}}(N) - \varepsilon_{N}^{\text{DFA}}(N), \tag{6.11}$$

where the superscript "DFA" means a conventional density functional approximation.

The appropriate framework for the prediction of the optical gap in exact KS is its TD linear response (i.e., TD KS) [45, 46]. Exact KS must predict the optical gap to be below the fundamental gap, in agreement with experiment, simply by virtue of being a formally exact theory. For semilocal functionals, the optical gap turns out to be [47–50]

$$\Delta E_{\text{og}}^{\text{SL}}(N) = \varepsilon_{N+1}^{\text{SL}}(N) - \varepsilon_{N}^{\text{SL}}(N). \tag{6.12}$$

In other words, semilocal functionals do not describe excitons, and predict the optical gap and fundamental gap to be the same. One must therefore not be dogmatic in claiming that the semilocal band energy difference constitutes a prediction for only one of the optical gap or fundamental gap. Due to self-interaction error, the occupied bands in semilocal DFT are too high in energy, and the semilocal optical gap severely underestimates the experimental optical gap. Thanks to the their nonlocal exchange component, global hybrids predict a nonzero exciton binding energy, and the quality of their prediction for the experimental optical or fundamental gap depends on the amount of nonlocal exchange they incorporate.

Because HSE is done in the generalized KS sense, the HSE band energy difference is the HSE fundamental gap. As a practical matter, the HSE band energy differences correspond better with the experimental optical gap than they do with the experimental fundamental gap, especially as the gap gets larger. Therefore in practice we claim that the HSE band energy difference should be understood as a prediction of

the experimental optical gap; because the optical and fundamental gaps are so close in semiconductors, for these systems the HSE band energy difference can also be used as a predictor of the experimental fundamental gap. As the gap gets larger, HSE band energy differences more dramatically underestimate the experimental fundamental gap, and as they get larger still, the HSE band energy difference becomes a poor predictor even for the experimental optical gap.

The success of HSE band energy differences can be rationalized quite straight-forwardly, once one knows a few properties of the parent semilocal global hybrid (PBEh) and its underlying GGA (PBE) [51]. As is typically the case for semilocal functionals, PBE band energy differences underestimate the gap. For semiconductors, the PBEh band energy differences overestimate the gap. One can think of HSE as an interpolation between PBE and PBEh; as the range-separation parameter ω varies between 0 and ∞, HSE varies between PBEh and PBE. Thus, there is some nonzero value of ω for which the HSE band energy difference reproduces the experimental gap. Schematically, this is illustrated in Figure 6.1. Note that because HSE includes a fraction of screened exact exchange, it has only a small exciton binding, so the TD HSE optical gap should not differ much from the band energy difference.

While it is reasonably clear that there should exist a value of ω that gives the correct gap for a given system, it is not so clear that this ω should be universal. In fact, it is not (see Ref. [52]). Nonetheless, $\omega = 0.11a_0^{-1}$ as used in HSE06 seems to be a reasonable system-averaged value across a wide variety of systems. The HSE band energy difference accurately reproduces the optical gap in semiconductors, but severely underestimates the gap in insulators, and the HSE band width in metallic systems is
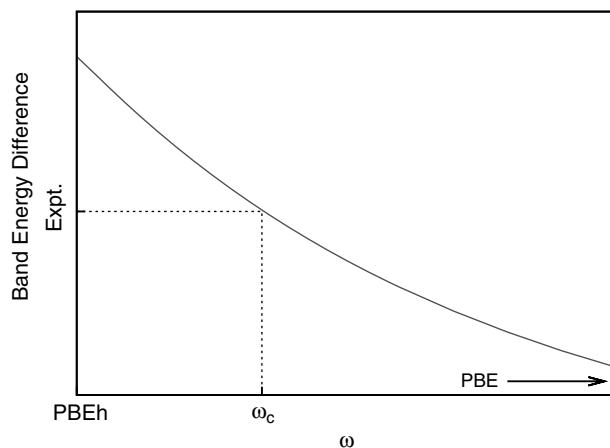
Figure 6.1 (online color at: www.pss-b.com) Schematic illustration of the ω-dependent band energy difference in HSE. The *x*-axis indicates that $\omega = 0$ corresponds to PBEh and $\omega \to \infty$ corresponds to PBE. The *y*-axis shows that the experimental gap lies between the PBE and PBEh band energy differences, so that there is some ω_C whose band energy difference reproduces the experimental gap.

generally too large [53, 54]. The failures of HSE for insulators and metals can be traced to the breakdown of the assumption that the PBE gap is too small and the PBEh gap is too large.

6.3
Screened Exchange

In this section we briefly outline a few important relations between the GW approximation, the closely related Coulomb-hole screened exchange (COHSEX) method, and screened hybrid functionals. The pragmatic justification for hybrid functionals is clear (HF and KS-DFT tend to err in opposite directions), as is the pragmatic justification for the use of screened hybrids (they make the calculation less expensive, and are more accurate in solids). There is, however, also a formal justification for screened hybrid DFT: the presence of the other electrons in the systems reduces the full, unscreened exchange used in HF to a certain (material-dependent) extent. We will shortly see that this screening is a direct consequence of the Coulomb correlation between the electrons. For a more rigorous discussion, we refer the reader to Ref. [55].

   As explained in Section 6.1, the HF method neglects Coulomb correlation entirely and therefore suffers from several shortcomings. This problem can be overcome by explicitly including correlation corrections. The GW approximation introduced by Hedin [56] in the context of many-body perturbation theory may help. Its name follows from the basic equation defining the frequency dependent self-energy $\Sigma(\omega)$ in terms of the interacting, frequency-dependent Green function $G(\omega)$ and the frequency-dependent *screened* Coulomb interaction $W(\omega)$:

$$\Sigma(\omega) = i\langle GW\rangle(\omega), \tag{6.13}$$

where $\langle GW\rangle$ indicates a convolution over the frequency ω'. Both G and W are nonlocal quantities. The physics is clearly seen by rewriting the screened Coulomb interaction:

$$\begin{aligned} W(\omega) &= \varepsilon^{-1}(\omega)v = \big(1 + v\chi(\omega)\big)v \\ &= v + W_{\mathrm{pol}}(\omega) \end{aligned} \tag{6.14}$$

using the dielectric function $\varepsilon^{-1}(\omega) = (1 + v\chi(\omega))$. The dielectric function in turn depends on the polarizability $\chi(\omega)$ and the "bare" (i.e., unscreened) Coulomb kernel $v = 1/|r_1 - r_2|$. The screened Coulomb interaction W can therefore be separated into an unscreened term v and the screened or polarizable term $W_{\mathrm{pol}} = v\chi v$, stemming from polarization of the electron density due to a small external potential [48]. Inserting Eq. (6.14) into Eq. (6.13) readily leads to

$$\Sigma(\omega) = iGv + i\langle GW_{\mathrm{pol}}\rangle(\omega) = \Sigma_{\mathrm{x}} + \Sigma_c(\omega), \tag{6.15}$$

demonstrating that the GW approximation goes beyond HF by inclusion of both exchange and correlation effects in the self-energy.

As suggested by Hedin (see Ref. [56]), ignoring the frequency dependence of Σ and taking care of a dependence on virtual orbitals in W_{pol} leads to the so-called static COHSEX approximation. The GW approximation is based on the random phase approximation (RPA) for ε^{-1}, which essentially means a diagrammatic ring or bubble graph expansion for the dielectric function [57]. For the homogeneous electron gas system, the static limit of RPA is the Thomas–Fermi (TF) approximation.[1] In Fourier space, the well known effective TF interaction is

$$W(\boldsymbol{q}, \omega = 0) = \frac{4\pi e^2}{\boldsymbol{q}^2 + k_{TF}^2}, \qquad\qquad k_{TF}^2 \sim r_s k_F^2, \qquad\qquad (6.16)$$

where r_s is known as the Wigner–Seitz radius and the Fermi wave-vector $k_F = (3\pi^2 n)^{1/3}$ (n is the electron density). Note that the TF interaction in real-space corresponds to the Yukawa potential (e^2/r) $e^{-k_{TF}r}$, where the effective screening length is determined by k_{TF}^{-1}. At first glance this can be seen as a route back to motivate the realization of a screened hybrid functional like HSE. Of course, the physics of metals does not directly apply to the physics of semiconductors and insulators. In insulators screening is "weaker" and the effective interaction has a more slowly decaying asymptotic behavior. However, closely related to the spirit of LDA, TF screening is commonly applied in so-called "screened exchange LDA" (SX-LDA) calculations using screened nonlocal exchange and LDA correlation potentials (see Ref. [30] and references therein). For further discussions and comparisons between the aforementioned SX calculations following Bylander and Kleinman [58] and HSE, we refer to Ref. [39].

6.4
Applications

Now that we have discussed some formal aspects of screened hybrid functionals like HSE, let us briefly touch on its performance for a variety of problems.

The success of HSE in the prediction of band gaps is well documented. As an example, Heyd *et al.* [59] considered a set of 40 solids of which 35 were semiconductors. After removing those solids for which the experimental gaps were either unavailable or larger than 4 eV, 28 semiconductors remain. Table 6.1 shows the predictions of HSE, LDA, PBE, and TPSS for the band gaps in the semiconductors in that set; the HSE numbers here use HSE06 and differ from those in Ref. [59]. While the semilocal functionals considerably underestimate the gap, HSE is quite accurate. Figure 6.2 shows a scatter plot of the HSE band gaps versus the experimental gaps (most of which are fundamental gaps, and which HSE generally underestimates slightly). These results were confirmed in plane-wave basis by Paier *et al.* [54] who also pointed out that HSE apparently includes too much exact exchange in metals (where it tends to overestimate band widths) [53] and too little in wide gap

---

[1] For small and large wave-vectors $\boldsymbol{q}$ in the high density limit; see, for example, Ref. [6].

Table 6.1 Mean error (ME) and mean absolute error (MAE) in the semiconductor band gaps for the SC 40 test set of Heyd *et al*. Results reported at the optimized geometry for each functional.

functional	ME (eV)	MAE (eV)
LSDA	−1.01	1.01
PBE	−0.98	0.98
TPSS	−0.83	0.83
HSE	−0.20	0.28

insulators, where it tends to underestimate the gap. As we have discussed, this is because HSE adopts a single, system-independent screening parameter ω which is most accurate for semiconductors. These same studies also demonstrated that HSE accurately predicts semiconductor lattice constants and gives improved estimates of bulk moduli.

Batista *et al*. [60] carried out a study on silicon, comparing several functionals (including HSE) to diffusion Monte Carlo (DMC), focusing on predictions for the formation energies of interstitial defects and on the relative stabilities of the diamond and β-tin phases. They found that LDA underestimates the defect formation energies by about 1.5 eV relative to the DMC results, while PBE underestimates them by about 1.0 eV. The TPSS meta-GGA is essentially no improvement on PBE. In sharp contrast to these semilocal functionals, HSE underestimates the DMC results by only 0.25 eV. Similar results are found for the relative stabilities of the diamond and β-tin phases; LDA, PBE, and TPSS underestimate the relative stability by roughly a factor of 2, but HSE is quite close to DMC (and in fact the two agree within the uncertainty of the DMC result). Figure 6.3 illustrates these results graphically.
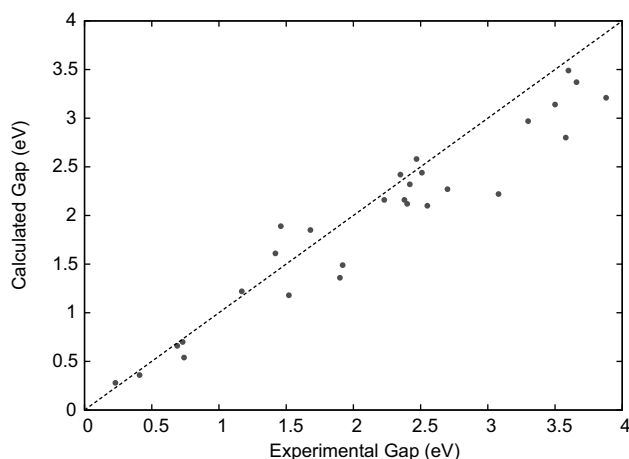
Figure 6.2 (online color at: www.pss-b.com) HSE band gap versus experimental band gap in the SC40 test set.
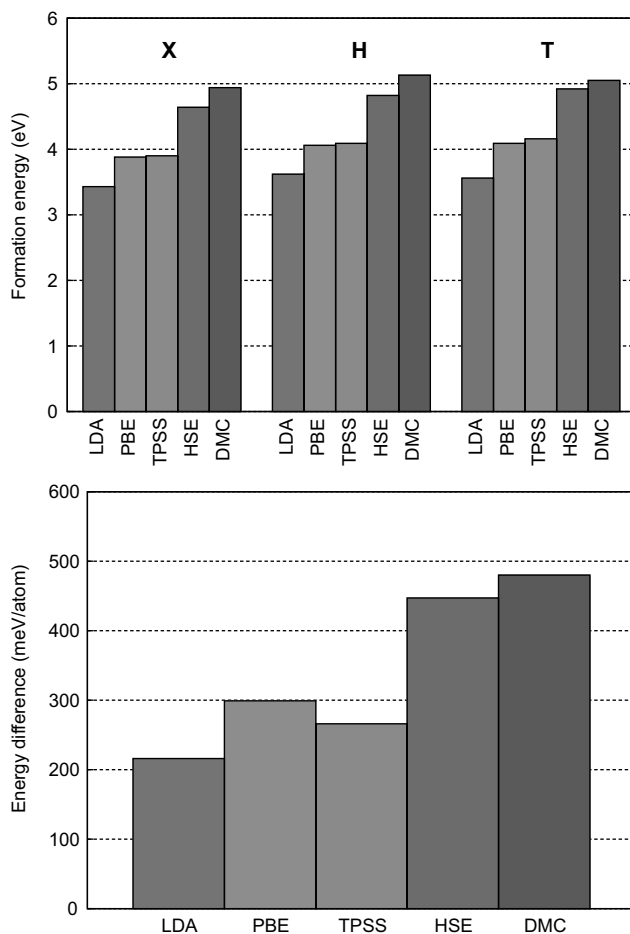
Figure 6.3 (online color at: www.pss-b.com) Comparison between DMC and several DFT functionals for the formation energy of X, H, and T interstitial defects (top panel) and for the relative stability of diamond and β-tin phases (bottom panel) in silicon.

In addition to these accurate results for semiconductors, HSE has properly described Mott insulators. Kasinathan *et al.* [61] showed that HSE correctly predicts the pressure-dependent Mott transition in MnO.

Lanthanide and actinide systems can be particularly challenging, since the *f* electrons are sometimes itinerant and other times localized. The balance between these possibilities leads to a multitude of possible ground states and phases. Semilocal functionals are not generally well suited for these systems because they do not properly describe localized states; this causes them to often give qualitatively incorrect results for band gaps and magnetic properties. On the other hand, HSE has had considerable success in describing rare earth systems, since its inclusion of screened exact exchange allows it treat itinerant and localized states in a balanced way.

Prodan *et al.* [62] studied UO_2, PuO_2, and β-Pu_2O_3. They showed that LDA and PBE incorrectly predict all three systems to be metallic, and TPSS is scarcely better, predicting the antiferromagnetic phases of PuO_2 and β-Pu_2O_3 to have a gap on the order of 0.05 eV. In contrast, HSE is qualitatively correct and provides reasonable gaps. While PBE and TPSS give reasonable lattice constants, HSE predicts essentially the exact result. The semilocal functionals predict that all three systems are ferromagnetic, while HSE correctly predicts that UO_2 and Pu_2O_3 are antiferromagnetic. The magnetic ordering of PuO_2 is controversial, but it is definitely not ferromagnetic and could be, as HSE predicts, antiferromagnetic.

Separate studies by Hay *et al.* [63], Da Silva *et al.* [64], and Ganduglia-Pirovano and coworkers [65] showed that HSE is particularly accurate for the structures of CeO_2 and Ce_2O_3, offering significant improvements over semilocal functionals. Semilocal functionals predict the ground state of Ce_2O_3 to be ferromagnetic, while HSE correctly predicts it to be antiferromagnetic. While HSE overestimates the gap for both CeO_2 and Ce_2O_3, it is significantly more accurate than are the semilocal functionals.

Another area where HSE has had considerable success is in the description of carbon nanotubes and graphene nanoribbons. Investigations have shown that HSE accurately predicts the optical excitation spectra of metallic nanotubes [66], and is also quite accurate for optical transitions in semiconducting nanotubes [67]. Additionally, HSE has been used to study the work function of nanotubes [68], as well as their polarizability [69, 70]. The electronic structure of graphene nanoribbons has also been considered [71, 72], and yield predictions that have been experimentally confirmed [73, 74].

Recently, Paier *et al.* [75] applied HSE and TD HSE to the potential photovoltaic material Cu_2ZnSnS_4. Their HSE results compare very favorably to experimental data for the lattice constants and the band gap, and the HSE band structure has been validated using the more expensive G_0W_0 quasiparticle calculations. Note that both HSE and previous absorption measurements coincide and predict the band gap to be on the order of 1.5 eV. This is in excellent agreement with an independent recent investigation by Chen *et al.* [76]. Note that HSE is much closer to experiment than PBE, the latter predicting a gap of 0.1 eV [75].

The HSE functional clearly outperforms conventional semilocal functionals for the description of defect transition levels. One important example is localizing acceptor levels in Cu_2O [77]. Chemical intuition suggests a localized Cu(I) $\rightarrow$ Cu(II) oxidation when creating an electron hole in the system. Semilocal functionals artificially delocalize the defect state, whereas HSE gives a very good description and produces defect transition levels in good agreement with experiment.

6.5
Conclusions

SX approximations are very powerful tools for density functional treatments of condensed systems. The HSE screened hybrid functional provides a computationally

efficient treatment of lattice parameters, bulk moduli, and band gaps of semiconductors and insulators, while incorporating only a single-empirical parameter. Interestingly, while this parameter was optimized for molecular atomization energies [31], it appears to contain universal information, as the same parameter yields semiconductor band gaps in excellent agreement with experiment. Because it includes a portion of nonlocal exchange and thereby partially alleviates the self-interaction error of semilocal functionals, HSE more correctly describes localized states. This is particularly relevant in the consideration of defects, where semilocal functionals will tend to incorrectly favor delocalized behavior.

The formal aspects of range-separated DFT exchange have been extensively investigated over decades, but several intellectually stimulating questions remain. One is to further elucidate the entanglement between correlation and exchange effects, or in other words, the mechanisms by which many-body correlations screen the exchange interaction. In particular, insights from many-body perturbation theory should help devise more effective screening models which can be applied to DFT. A single range-separation parameter seems sufficient to describe most of the physics we need for semiconductors, but additional flexibility seems to be important if the same functional is also to describe metals or insulators. A straightforward way to add this flexibility is to add additional ranges in what we would term a multirange hybrid [78, 79]. In order to more completely incorporate the physics of SX, one might consider position-dependent fractions of exact exchange [80–87] or position-dependent range separation [88, 89] in successors to HSE. Nonempirical treatments of these quantities are desirable, and should be provided by connections to many-body theory.

Acknowledgements

References

1 Ruzsinszky, A., Perdew, J.P., Csonka, G.I., Vydrov, O.A., and Scuserua, G.E. (2006) *J. Chem. Phys.*, **125**, 194112.

2 Mori-Sánchez, P. and Cohen, A.J. (2006) *J. Chem. Phys.*, **125**, 201102.

3 Mori-Sánchez, P., Cohen, A.J., and Yang, W. (2008) *Phys. Rev. Lett.*, **100**, 146401.

4 Monkhorst, H.J. (1979) *Phys. Rev. B*, **20**, 1504.

5 Parr, R.G. and Yang, W. 1989 *Density Functional Theory of Atoms and Molecules* (Oxford University Press, New York).

6 Dreizler, R.M. and Gross, E.K.U. (1995) *Density Functional Theory* (Plenum Press, New York).

7 Scuseria, G.E. and Staroverov, V.N. (2005) in: *Theory and Applications of Computational Chemistry: The First 40 Years,* (eds C.E., Dykstra, G., Frenking,

K.S., Kim, and G.E., Scuseria), Elsevier, Amsterdam, The Netherlands, pp. 669–724.

8 Sharp, R.T. and Horton, G.K. (1953) *Phys. Rev.*, **90**, 317.

9 Talman, J.D. and Shadwick, W.F. (1976) *Phys. Rev. A*, **14**, 36.

10 Staroverov, V.N., Scuseria, G.E., and Davidson, E.R. (2006) *J. Chem. Phys.*, **124**, 141103.

11 Sala, F.D. and Görling, A. (2001) *J. Chem. Phys.*, **115**, 5718.

12 Gritsenko, O.V. and Baerends, E.J. (2001) *Phys. Rev. A.*, **64**, 042506.

13 Grüning, M., Gritsenko, O.V., and Baerends, E.J. (2002) *J. Chem. Phys.*, **116**, 6435.

14 Staroverov, V.N., Scuseria, G.E., and Davidson, E.R. (2006) *J. Chem. Phys.*, **125**, 081104.

15 Izmaylov, A.F., Staroverov, V.N., Scuseria, G.E., and Davidson, E.R. (2007) *J. Chem. Phys.*, **127**, 084113.

16 Bulat, F.A. and Levy, M. (2009) *Phys. Rev. A*, **80**, 052510.

17 Perdew, J.P., Burke, K., and Ernzerhof, M. (1996); *Phys. Rev. Lett.*, **77**, 3865; *Phys. Rev. Lett.*, **78**, 1396(E) (1997).

18 Perdew, J.P. and Wang, Y. (1986) *Phys. Rev. B*, **33**, 8800; *Phys. Rev. B*, **40**, 3399(E) (1989).

19 Perdew, J.P., Burke, K., and Wang, Y. (1996) *Phys. Rev. B*, **54**, 16533.

20 Tao, J., Perdew, J.P., Staroverov, V.N., and Scuseria, G.E. (2003) *Phys. Rev. Lett.*, **91**, 146401.

21 Perdew, J.P., Ruzsinszky, A., Csonka, G.I., Vydrov, O.A., Scuseria, G.E., Constantin, L.A., Zhou, X., and Burke, K. (2008) *Phys. Rev. Lett.*, **100**, 136406; Erratum: *Phys. Rev. Lett.*, **102**, 039902 (2009).

22 Perdew, J.P., Ruzsinszky, A., Csonka, G.I., Constantin, L.A., and Sun, J. (2009) *Phys. Rev. Lett.*, **103**, 026403.

23 Cohen, A.J., Mori-Sánchez, P., and Yang, W. (2008) *Phys Rev. B*, **77**, 115123.

24 Becke, A.D. (1993) *J. Chem. Phys.*, **98**, 1372.

25 Becke, A.D. (1993) *J. Chem. Phys.*, **98**, 5648.

26 Stephens, P.J., Devlin, F.J., Chabalowski, C.F., and Frisch, M.J. (1994) *J. Phys. Chem.*, **98**, 11623.

27 Perdew, J.P., Ernzerhof, M., and Burke, K. (1996) *J. Chem. Phys.*, **105**, 9982.

28 Ernzerhof, M. and Scuseria, G.E. (1999) *J. Chem. Phys.*, **110**, 5029.

29 Adamo, C. and Barone, V. (1999) *J. Chem. Phys.*, **110**, 6158.

30 Seidl, A., Görling, A., Vogl, P., Majewski, J.A., and Levy, M. (1996) *Phys. Rev. B*, **53**, 3764.

31 Heyd, J., Scuseria, G.E., and Ernzerhof, M. (2003) *J. Chem. Phys.*, **118**(18), 8207.

32 Heyd, J. and Scuseria, G.E. (2004) *J. Chem. Phys.*, **120**, 7274.

33 Heyd, J. and Scuseria, G.E. (2004) *J. Chem. Phys.*, **121**, 1187.

34 Heyd, J., Scuseria, G.E., and Ernzerhof, M. (2006) *J. Chem. Phys.*, **124**, 219906.

35 Henderson, T.M., Izmaylov, A.F., Scalmani, G., and Scuseria, G.E. (2009) *J. Chem. Phys.*, **131**, 044108.

36 Savin, A. and Flad, H.J. (1995) *Int. J. Quantum Chem.*, **56**, 327.

37 Leininger, T., Stoll, H., Werner, H.J., and Savin, A. (1997) *Chem. Phys. Lett.*, **275**, 151.

38 Savin, A. (1996) in: *Recent Developments and Applications of Modern Density Functional Theory*, (ed. J.M. Seminario), Elsevier, Amsterdam, The Netherlands, pp. 327–357.

39 Janesko, B.G., Henderson, T.M., and Scuseria, G.E. (2009) *Phys. Chem. Chem. Phys.*, **11**, 443.

40 Hanke, W. (1978) *Adv. Phys.*, **27**, 287.

41 Bruneval, F., Sottile, F., Olevano, V., and Reining, L. (2006) *J. Chem. Phys.*, **124**, 144113.

42 Janak, J.F. (1978) *Phys. Rev. B*, **18**, 7165.

43 Perdew, J.P. and Levy, M. (1983) *Phys. Rev. Lett.*, **51**, 1884.

44 Sham, L.J. and Schlüter, M. (1983) *Phys. Rev. Lett.*, **51**, 1888.

45 Gross, E.K.U. and Dreizler, R.M. (eds.), *Density Functional Theory II* (Springer, Heidelberg, 1996).

46 Casida, M.E. (1995) in: *Recent Advances in Density Functional Methods, Part I*, (ed. D.P., Chong), World Scientific, Singapore, p. 155.

47 Hirata, S., Head-Gordon, M., and Bartlett, R.J. (1999) *J. Chem. Phys.*, **111**, 10774.

48 Onida, G., Reining, L., and Rubio, A. (2002) *Rev. Mod. Phys.*, **74**, 601.

49 Botti, S., Schindlmayr, A., Sole, R.D., and Reining, L. (2007) *Rep. Prog. Phys.*, **70**, 357.

50 Izmaylov, A.F. and Scuseria, G.E. (2008) *J. Chem. Phys.*, **129**, 034101.

51 Brothers, E.N., Izmaylov, A.F., Normand, J.O., Barone, V., and Scuseria, G.E. (2008) *J. Chem. Phys.*, **129**, 011102.

52 Paier, J., Marsman, M., and Kresse, G. (2008) *Phys. Rev. B*, **78**, 121201.

53 Stroppa, A., Termentzidis, K., Paier, J., Kresse, G., and Hafner, J. (2007) *Phys. Rev. B*, **76**, 195440.

54 Paier, J., Marsman, M., Hummer, K., Kresse, G., Gerber, I.C., and Ángyán, J.A. (2006) *J. Chem. Phys.*, **124**, 154709; Erratum: *J. Chem. Phys.*, **125**, 249901 (2006).

55 Del-Sole, R., Reining, L., and Godby, R.W. (1994) *Phys. Rev. B*, **49**, 8024.

56 Hedin, L. (1965) *Phys. Rev.*, **139**, A796.

57 Hedin, L. (1999) *J. Phys.: Condens. Matter*, **11**, R489.

58 Bylander, D.M. and Kleinman, L. (1990) *Phys. Rev. B*, **41**, 7868.

59 Heyd, J., Peralta, J.E., Scuseria, G.E., and Martin, R.L. (2005) *J. Chem. Phys.*, **123**, 174101.

60 Batista, E., Heyd, J., Hennig, R.G., Uberuaga, B.P., Margin, R.L., Scuseria, G.E., Umrigar, C.J., and Wilkins, J.W. (2006) *Phys. Rev. B*, **74**, 121102.

61 Kasinathan, D., Kunes, J., Koepernik, K., Diaconu, C.V., Martin, R., Prodan, I.D., Scuseria, G.E., Spaldin, N., Petit, L., Schulthess, T.C., and Pickett, W.E. (2006) *Phys. Rev. B*, **74**, 195110.

62 Prodan, I.D., Scuseria, G.E., and Martin, R.L. (2007) *Phys. Rev. B*, **76**, 033101.

63 Hay, P.J., Martin, R.L., Uddin, J., and Scuseria, G.E. (2006) *J. Chem. Phys.*, **125**, 034712.

64 Da Silva, J. L. F., Ganduglia-Pirovano, M.V., Sauer, J., Bayer, V., and Kresse, G. (2007) *Phys. Rev. B*, **75**, 045121.

65 Ganduglia-Pirovano, M.V., Da Silva, J., and Sauer, J. (2009) *Phys. Rev. Lett.*, **102**, 026101.

66 Barone, V., Peralta, J.E., and Scuseria, G.E. (2005) *Nano Lett.*, **5**, 1830.

67 Barone, V., Peralta, J.E., Wert, M., Heyd, J., and Scuseria, G.E. (2005) *Nano Lett.*, **5**, 1621.

68 Barone, V., Peralta, J.E., Uddin, J., and Scuseria, G.E. (2006) *J. Chem. Phys.*, **124**, 024709.

69 Brothers, E.N., Scuseria, G.E., and Kudin, K.N. (2006) *J. Phys. Chem. B*, **110**, 12860.

70 Brothers, E.N., Izmaylov, A.F., Scuseria, G.E., and Kudin, K.N. (2008) *J. Phys. Chem. C*, **112**, 1396.

71 Ezawa, M. (2006) *Phys. Rev. B*, **73**, 045432.

72 Barone, V., Hod, O., and Scuseria, G.E. (2006) *Nano Lett.*, **6**, 2748.

73 Hand, M.Y., Özyilmaz, B., Zhang, Y., and Lim, P. (2007) *Phys. Rev. Lett.*, **98**, 206805.

74 Chen, Z., Lu, Y.M., Rooks, M.J., and Avouris, P. (2007) *Physica E*, **40**, 228.

75 Paier, J., Asahi, R., Nagoya, A., and Kresse, G. (2009) *Phys. Rev. B*, **79**, 115126.

76 Chen, S., Gong, X.G., Walsh, A., and Wei, S.H. (2009) *Appl. Phys. Lett.*, **94**, 041903.

77 Scanlon, D.O., Morgan, B.J., Watson, G.W., and Walsh, A. (2009) *Phys. Rev. Lett.*, **103**, 096405.

78 Henderson, T.M., Izmaylov, A.F., Scuseria, G.E., and Savin, A. (2007) *J. Chem. Phys.*, **127**, 221103.

79 Henderson, T.M., Izmaylov, A.F., Scuseria, G.E., and Savin, A. (2008) *J. Theor. Comput. Chem.*, **4**, 1254.

80 Burke, K., Cruz, F.G., and Lam, K.C. (1998) *J. Chem. Phys.*, **109**, 8161.

81 Jaramillo, J., Scuseria, G.E., and Ernzerhof, M. (2003) *J. Chem. Phys.*, **118**, 1068.

82 Janesko, B.G. and Scuseria, G.E. (2007) *J. Chem. Phys.*, **127**, 164117.

83 Bahmann, H., Rodenberg, A., Arbuznikov, A.V., and Kaupp, M. (2007) *J. Chem. Phys.*, **126**, 011103.

84 Arbuznikov, A.V. and Kaupp, M. (2007) *Chem. Phys. Lett.*, **440**, 160.

85 Kaupp, M., Bahmann, H., and Arbuznikov, A.V. (2007) *J. Chem. Phys.*, **127**, 194102.

86 Janesko, B.G. and Scuseria, G.E. (2008) *J. Chem. Phys.*, **128**, 084111.

87 Haunschild, R., Janesko, B.G., and Scuseria, G.E. (2009) *J. Chem. Phys.*, **131**, 154112.

88 Krukau, A.V., Scuseria, G.E., Perdew, J.P., and Savin, A. (2008) *J. Chem. Phys.*, **129**, 124103.

89 Henderson, T.M., Janesko, B.G., Scuseria, G.E., and Savin, A. (2009) *J. Quantum Chem.*, **109**, 2023.